Geophysical Research Letters

Supporting Information for

Venus: A Thick Basal Magma Ocean May Exist Today

J. G. O'Rourke

School of Earth and Space Exploration, Arizona State University, Tempe, AZ, USA

Contents of this file

Text S1.

This section provides the equations that govern the models for Earth and Venus. Full descriptions are available from Labrosse et al. (2017), O'Rourke et al. (2018), and cited references therein. Wherever possible, this study copies the notation of prior publications. The code used to run the models and generate all figures is publicly available as stated in the Acknowledgements.

S1.1. General methods

The global energy budget for the coupled evolution of the BMO and the core is

$$Q_{BMO} = Q_{SM} + Q_{RM} + Q_{LM} + Q_{CMB}, \quad (S1)$$

where the heat flow across the solid/liquid interface in the basal mantle (Q_{BMO}) equals the sum of the radiogenic heating in the BMO (Q_{RM}), the secular cooling of the BMO (Q_{SM}), the latent heat released by solidification of the BMO (Q_{LM}), and the heat flow across the core/mantle boundary (Q_{CMB}). Next, the energy budget of the core is expanded as

$$Q_{CMB} = Q_{SC} + Q_{RC} + Q_{PC} + Q_{GC} + Q_{LC} + Q_{IC}, \quad (S2)$$

which includes secular cooling of the outer core (Q_{SC}), radiogenic heating (Q_{RC}), precipitation of Mg-rich minerals near the CMB (Q_{PC}), and three terms associated with the growth of an inner core: gravitational energy from excluded light elements (Q_{GC}), latent heat (Q_{LC}), and conductive cooing (Q_{IC}). Combining the contributions from individual isotopes in the BMO,

$$Q_{RM} = Q_{RM}(0)\exp[-\lambda_M t], \quad (S3)$$

where $Q_{RM}(0)$ is the initial radiogenic heat production in the BMO and λ_M is an average decay constant. Crucially, we assume that heat-producing elements are incompatible in the solidifying mantle so the volumetric heating rate in the BMO increases over time. Assuming that potassium is the only source of radiogenic heat in the core,

$$Q_{RC} = M_C H_K [K]_C \exp(-\lambda_C t), \quad (S4)$$

where M_C is the mass of the core, H_K is the initial radiogenic heat production per unit mass per ppm of potassium, $[K]_C$ is the abundance of potassium in the core, and λ_M is the decay constant for potassium-40.

All other terms on the right-hand sides of Eq. 1 and 2 are proportional to the cooling rate of the core and BMO (Labrosse, 2015; O'Rourke et al., 2018). That is,

$$Q_i = \tilde{Q}_i \left(\frac{dT_C}{dt}\right). \quad (S5)$$

Combining Eq. 1, 2, and 5 yields

$$\frac{dT_C}{dt} = \frac{Q_{BMO} - Q_{RM} - Q_{RC}}{\tilde{Q}_{SM} + \tilde{Q}_{LM} + \tilde{Q}_{SC} + \tilde{Q}_{PC} + \tilde{Q}_{GC} + \tilde{Q}_{LC} + \tilde{Q}_{IC}}. \quad (S6)$$

Crucially, the numerator of the right side of this equation is easily calculated from the imposed boundary condition for the model (Q_{BMO}) and two initial conditions (Q_{RM} and Q_{RC}). The key to obtaining a thermal history is then to write the proportionalities in the denominator as functions of the thermodynamic properties of the BMO and the core (Labrosse, 2015).

S1.1.1. Evolution of the BMO

S1.1.1.1. Heat budget

The boundary condition for the model is the heat flow out of the BMO into the solid mantle (Q_{BMO}), which we impose as a linear function of time:

$$Q_{BMO}(t) = Q_{BMO}(t_p) + \Delta Q_{BMO}\left(\frac{t - t_p}{t_p}\right), \quad (S7)$$

where t_p is the time at present day. The resultant rate of secular cooling in the BMO is

$$\tilde{Q}_{SM} = -M_M C_M, \quad (S8)$$

where M_M is the mass of the basal magma ocean and C_M is its specific heat (Labrosse et al., 2007).

The solidification rate of the BMO is directly proportional to its cooling rate. We assume a linear phase diagram: $T_C = T_A - (T_A - T_B)\phi_L$, where ϕ_L is the concentration of the Fe-rich endmember (Labrosse et al., 2007). The liquidus temperature is T_A and T_B when ϕ_L equals 0 and 1, respectively. Differentiating both sides of that equation, $dT_C/dt = -(T_A - T_B)d\phi_L/dt$, which shows that fractional crystallization increases the Fe content of the BMO. Conservation of chemical species implies

$$\frac{d\phi_L}{dt} = -\frac{3r_B^2\Delta\phi}{r_B^3 - r_C^3}\left(\frac{dr_B}{dt}\right), \quad (S9)$$

where $\Delta\phi$ is the Fe-enrichment of the BMO relative to the solid mantle (Labrosse et al., 2007). Therefore,

$$\frac{dT_C}{dt} = \frac{3r_B^2\Delta\phi(T_A - T_B)}{r_B^3 - r_C^3}\left(\frac{dr_B}{dt}\right). \quad (S10)$$

Finally, the latent heat is proportional to ΔS_M, the specific entropy of melting for the BMO (Labrosse et al., 2007):

$$\tilde{Q}_{LM} = -4\pi r_B^2\Delta S_M\rho_M T_C\left(\frac{r_B^3 - r_C^3}{3r_B^2\Delta\phi(T_A - T_B)}\right). \quad (S11)$$

S1.1.1.2. Dynamo criterion

Vigorous convection in the BMO may produce a dynamo. The magnetic Reynolds number is $Rm = \mu_0 v_M h_M \sigma_M$, where μ_0 is the permittivity of free space, v_M is the convective velocity, and σ_M is electrical conductivity (Blanc et al., 2019; Ziegler & Stegman, 2013). A dynamo may exist if $Rm > O(10)$. Three expressions for v_M are available (Christensen, 2010):

$$v_{MLT} = \left(\frac{h_M Q_{BMO}}{\rho_M H_T}\right)^{\frac{1}{3}} \quad (S12)$$

from mixing length theory,

$$v_{CIA} = \left(\frac{Q_{BMO}}{\rho_M H_T}\right)^{\frac{2}{5}}\left(\frac{h_M}{\Omega}\right)^{\frac{1}{5}} \quad (S13)$$

from the Coriolis-Inertial-Archimedean (CIA) force balance, and

$$v_{MAC} = \left(\frac{Q_{BMO}}{\Omega\rho_M H_T}\right)^{\frac{1}{2}} \quad (S14)$$

from the Magnetic-Archimedean-Coriolis (MAC) force balance. Here Ω is the rotational rate of the planet and $H_T = C_M/(\alpha_M g)$ is the thermal scale height with α_M as the coefficient of thermal expansion and g as the gravitational acceleration in the BMO. The magnetic field strength within the BMO is approximately

$$B_M = (2\epsilon f_{ohm}\mu_0\rho_M v_M^2)^{\frac{1}{2}}, \quad (S15)$$

where ε is a constant prefactor and f_{ohm} is the fraction of available power that is converted to ohmic dissipation as magnetic energy. Finally, the magnetic field strength at the surface is

$$B_S = \frac{1}{7}B_M\left(\frac{r_B}{r_P}\right)^3. \quad (S16)$$

S1.1.2. Evolution of the core

S1.1.2.1. Structure and heat budget

Following many previous studies (e.g., Labrosse, 2015; O'Rourke et al., 2018, 2017), the density of the core is parameterized with a fourth-order polynomial:

$$\rho(r) = \rho_0 \left[1 - \left(\frac{r}{L_p}\right)^2 - A_p \left(\frac{r}{L_p}\right)^4\right], \quad (S17)$$

where ρ_0 is the central density, r is radial distance, $L_p = [3K/(2\pi G\rho_0^2)]^{1/2}$ is a characteristic length scale, and $A_p = 0.5K' - 1.3$ is constant. Here G is the gravitational constant, K is an effective modulus, and K' is its effective derivative. The adiabatic temperature profile in the core is

$$T_a(r) = T_0 \left[1 - \left(\frac{r}{L_p}\right)^2 - A_p \left(\frac{r}{L_p}\right)^4\right]^{\gamma}, \quad (S18)$$

where T_0 is the central temperature and γ is the Grüneisen parameter. Integrating these profiles over the core results in gnarly polynomial expressions for terms involved in the global energy balance. To simplify those expressions, four useful functions are defined:

$$f_c(x,\delta) = x^3\left[1 - \frac{3}{5}(\delta+1)x^2 - \frac{3}{14}(\delta+1)\left(2A_p - \delta\right)x^4\right], \quad (S19)$$

$$f_k(x) = 0.2x^5\left[1 + \frac{10}{7}\left(1+2A_p\right)x^2 + \frac{5}{9}\left(3 + 10A_p + 4A_p^2\right)x^4\right], \quad (S20)$$

$$f_\chi(x) = x^3\left\{-\frac{1}{3}\left(\frac{r_I}{L_p}\right)^2 - \frac{1}{2}\left[1 + \left(\frac{r_I}{L_p}\right)^2\right]x^2 - \frac{13}{70}x^4\right\}, \quad (S21)$$

and

$$f_\gamma(x) = x^3\left[-\frac{\Gamma}{3} + \left(\frac{1+\Gamma}{5}\right)x^2 + \left(\frac{A_p\Gamma - 1.3}{7}\right)x^4\right], \quad (S22)$$

where

$$\Gamma = \left(\frac{r_C}{L_p}\right)^2\left[1 - \frac{1}{3}\left(\frac{r_C}{L_p}\right)^2\right]. \quad (S23)$$

An inner core nucleates once the adiabatic temperature at the center of the core drops below the liquidus and grows over time. The liquidus temperature in the outer core increases with pressure but decreases as more light elements are added (Labrosse, 2015):

$$T_L(r) = T_L(0) - K\left(\frac{dT_L}{dP}\right)\left(\frac{r_I}{L_p}\right)^2 + \frac{c_0\left(\frac{dT_L}{dc}\right)}{f_c\left(\frac{r_C}{L_p}, 0, A_p\right)}\left(\frac{r_I}{L_p}\right)^3, \quad (S24)$$

where dT_L/dP and dT_L/dc are the changes in liquidus temperature with pressure and composition, respectively, and c_0 is the initial concentration of light elements in the core. Before the inner core grows, the secular cooling of the core is expressed as

$$\tilde{Q}_{SC} = -\frac{4}{3}\pi\rho_0 C_C L_p^3 f_c\left(\frac{r_C}{L_p}, \gamma\right)\left[1 - \left(\frac{r_C}{L_p}\right)^2 - A_p\left(\frac{r_C}{L_p}\right)^4\right]^{-\gamma}. \quad (S25)$$

After the inner core nucleates, the secular cooling term is more complicated (Labrosse, 2015):

$$\tilde{Q}_{SC} = -\frac{4}{3}\pi\rho_0 C_C L_p^3 \left[1 - \left(\frac{r_I}{L_p}\right)^2 - A_p\left(\frac{r_I}{L_p}\right)^4\right]^{-\gamma} \left[\frac{dT_L}{dr_I} + \frac{2\gamma T_L(r_I)\left(\frac{r_I}{L_p^2}\right)\left(1 + 2A_p\left(\frac{r_I}{L_p}\right)^2\right)}{1 - \left(\frac{r_I}{L_p}\right)^2 - A_p\left(\frac{r_I}{L_p}\right)^4}\right]\left[f_c\left(\frac{r_C}{L_p}, \gamma\right) - f_c\left(\frac{r_I}{L_p}, \gamma\right)\right]\left(\frac{dr_I}{dT_C}\right). \quad (S26)$$

The liquidus temperature at the inner core boundary is

$$T_L(r_I) = T_L(0) - \left[K\left(\frac{dT_L}{dP}\right)\left(\frac{r_I}{L_p}\right)^2 + \frac{c_0\left(\frac{dT_L}{dc}\right)r_I^3}{L_p^3 f_c\left(\frac{r_C}{L_p}, 0\right)}\right], \quad (S27)$$

which is differentiated to obtain the slope of the liquidus at the inner core boundary:

$$\frac{dT_L}{dr_I} = -2\left[K\left(\frac{dT_L}{dP}\right)\left(\frac{r_I}{L_p^2}\right) + \frac{3c_0\left(\frac{dT_L}{dc}\right)r_I^2}{L_p^3 f_c\left(\frac{r_C}{L_p}, 0\right)}\right]. \quad (S28)$$

Likewise, the growth rate of the inner core is proportional to the cooling rate (Nimmo, 2015; O'Rourke et al., 2017, 2018):

$$\frac{dr_I}{dT_C} = -\frac{1}{\left(\frac{dT_L}{dP} - \frac{dT_a}{dP}\right)_{r_I}}\left(\frac{T_L(r_I)}{T_C\rho_I g_I}\right), \quad (S29)$$

where ρ_I and g_I are the density and gravitational acceleration at the inner core boundary, respectively. The adiabatic temperature gradient at the inner core boundary is $\mathrm{d}T_a/\mathrm{d}P = \gamma T_L(r_I)/K$. The gravitational energy associated with the exclusion of light elements from the inner core is

$$\tilde{Q}_{GC} = \frac{8\pi^2 G\rho_0 c_0 \alpha_I r_I^2 L_p^2}{f_c\left(\frac{r_C}{L_p}, 0\right)}\left[f_\chi\left(\frac{r_C}{L_p}\right) - f_\chi\left(\frac{r_I}{L_p}\right)\right]\left(\frac{dr_I}{dT_C}\right). \quad (S30)$$

Next, the latent heat of solidification released from the inner core is

$$\tilde{Q}_{LC} = 4\pi r_I^2 \rho_I T_L(r_I)\Delta S_C\left(\frac{dr_I}{dT_C}\right), \quad (S31)$$

where ΔS_C is the entropy of melting for the core. Assuming the inner core conducts heat efficiently, the conductive heat flow across the inner core boundary is

$$\tilde{Q}_{IC} = C_C M_I K\left(\frac{dT_L}{dP}\right)\left(\frac{2r_I}{L_p^2} + \frac{16r_I}{5L_p^5}\right)\left(\frac{dr_I}{dT_C}\right), \quad (S32)$$

where M_I is the mass of the inner core. In the core, the mass enclosed within a certain radius is

$$M(r) = \frac{4}{3}\pi\rho_0 L_p^3 f_c\left(\frac{r}{L_p}, 0\right). \quad (S33)$$

Finally, the gravitational energy produced by the precipitation of light elements at the CMB is

$$\tilde{Q}_{PC} = \frac{8}{3}\pi G\rho_0^2 L_p^5 \alpha_P P_C\left[f_\gamma\left(\frac{r_C}{L_p}\right) - f_\gamma\left(\frac{r_I}{L_p}\right)\right]. \quad (S34)$$

S1.1.2.1. Dynamo criterion

The strength of any core-hosted dynamo is predicted with scaling laws from previous studies based on the total energetic dissipation (O'Rourke et al., 2018). In contrast to the model for the

BMO, convective velocities in the core are not explicitly computed. Instead, the total dissipation is calculated as $\Phi = \Phi_i + \Phi_o$, where Φ_i and Φ_o are contributions from the inner core boundary and the CMB, respectively. Each contribution includes the energetic terms from Eq. 2 multiplied by an efficiency factor (Aubert et al., 2009; Labrosse, 2015):

$$\Phi_i = \frac{T_{DC}[T_L(r_I) - T_C]}{T_L(r_I)T_C}(Q_{LC} + Q_{IC}) + \frac{T_{DC}}{T_C}(Q_{GC}) \quad (S35)$$

and

$$\Phi_o = \frac{T_{DC} - T_C}{T_C}(Q_{RC}) + \frac{T_{DC}(T_{SC} - T_C)}{T_{SC}T_C}(Q_{SC}) + \frac{T_{DC}}{T_C}(Q_{PC}) - T_{DC}E_K. \quad (S36)$$

The effective temperatures for uniform dissipation and secular cooling are, respectively,

$$T_{DC} = \frac{T(r_I)}{\left[1 - \left(\frac{r_I}{L_p}\right)^2 - A_p\left(\frac{r_I}{L_p}\right)^4\right]^\gamma}\left[\frac{f_c\left(\frac{r_C}{L_p}, 0\right) - f_c\left(\frac{r_I}{L_p}, 0\right)}{f_c\left(\frac{r_C}{L_p}, -\gamma\right) - f_c\left(\frac{r_I}{L_p}, -\gamma\right)}\right], \quad (S37)$$

and

$$T_{SC} = \frac{T(r_I)}{\left[1 - \left(\frac{r_I}{L_p}\right)^2 - A_p\left(\frac{r_I}{L_p}\right)^4\right]^\gamma}\left[\frac{f_c\left(\frac{r_C}{L_p}, \gamma\right) - f_c\left(\frac{r_I}{L_p}, \gamma\right)}{f_c\left(\frac{r_C}{L_p}, 0\right) - f_c\left(\frac{r_I}{L_p}, 0\right)}\right]. \quad (S38)$$

Although $T_{DC} \sim T_{SC}$ within <10 K, $T_{DC} < T_{SC}$ because the dissipation associated with secular cooling is generated near the CMB, meaning that secular cooling is a slightly more efficient power source for the dynamo than radiogenic heating. Gravitational energy terms (Q_{PC} and Q_{GC}) are even more efficient because those dissipation terms are not penalized by a "Carnot-like" efficiency. The entropy sink associated with thermal conduction in the core is

$$E_K = 16\pi\gamma^2 k_C L_p\left[f_k\left(\frac{r_C}{L_p}\right) - f_k\left(\frac{r_I}{L_p}\right)\right], \quad (S39)$$

where k_C is the thermal conductivity of the core. Then we define the convective power as $P = \Phi/[M_C\Omega^3(r_C - r_I)^2]$ (Aubert et al., 2009). The rms magnetic field in the core is $B_{rms} = 1.5\Omega(r_C - r_I)P^{0.34}(\rho\mu_0)^{1/2}$ (Aubert et al., 2009). Next, we calculate the gravitational potentials at the CMB, inner core boundary, and on average in the outer core as $\varphi_C = r_C g/2$, $\varphi_I = r_I^2 g/(2r_C)$, and $\varphi_{av} = 0.3(g/r_C)[(r_C^5 - r_I^5)/(r_C^3 - r_I^3)]$, respectively (Aubert et al., 2009). The mass fluxes attributable to dissipation at the inner core boundary and CMB are $F_I = \Phi_I/(\varphi_{av} - \varphi_I)$ and $F_O = \Phi_O/(\varphi_O - \varphi_{av})$, respectively, and then $f_I = F_I/(F_I + F_O)$ (Aubert et al., 2009). The ratio $b_{dip} = 7.3(1 - r_I/r_C)(1+f_I)$ expresses the strength of the internal field relative to the dipole field at the CMB. The true dipole moment (TDM) is calculated (Aubert et al., 2009):

$$\mathrm{TDM} = \frac{4\pi r_C^3}{\sqrt{2}\mu_0}\left(\frac{B_{rms}}{b_{dip}}\right). \quad (S40)$$

Finally, the magnetic field at the equator is $B_S = \mu_0 \mathrm{TDM}/(4\pi r_P^3)$.

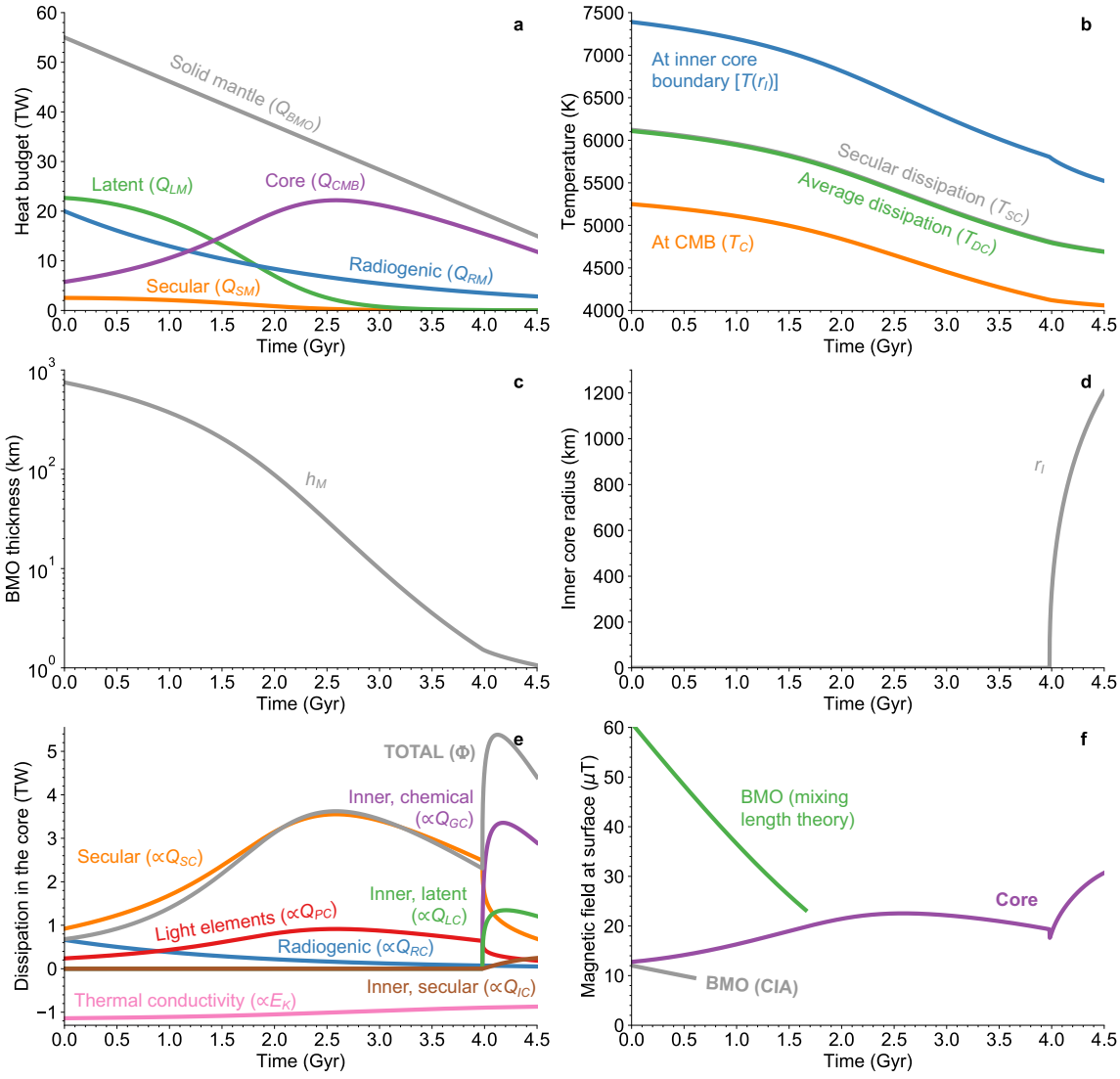

180

181 **Figure S1.** Nominal model for Earth discussed in Section 3.1 of the main text. A basal magma
182 ocean survives for billions of years but is almost completely solidified at present day, which
183 obeys seismic constraints. (a) Heat budget of the basal magma ocean. (b) Temperatures at the
184 core/mantle boundary and deeper in the core. (c) Thickness of the basal magma ocean. (d) Radius
185 of the inner core. (e) Dissipation budget for the core. (f) Estimated strength of the magnetic field
186 at the surface based on the scaling law for the core and two velocity scalings for the basal magma
187 ocean. The MAC-scaling for the basal magma ocean predicts a field strength of zero always.

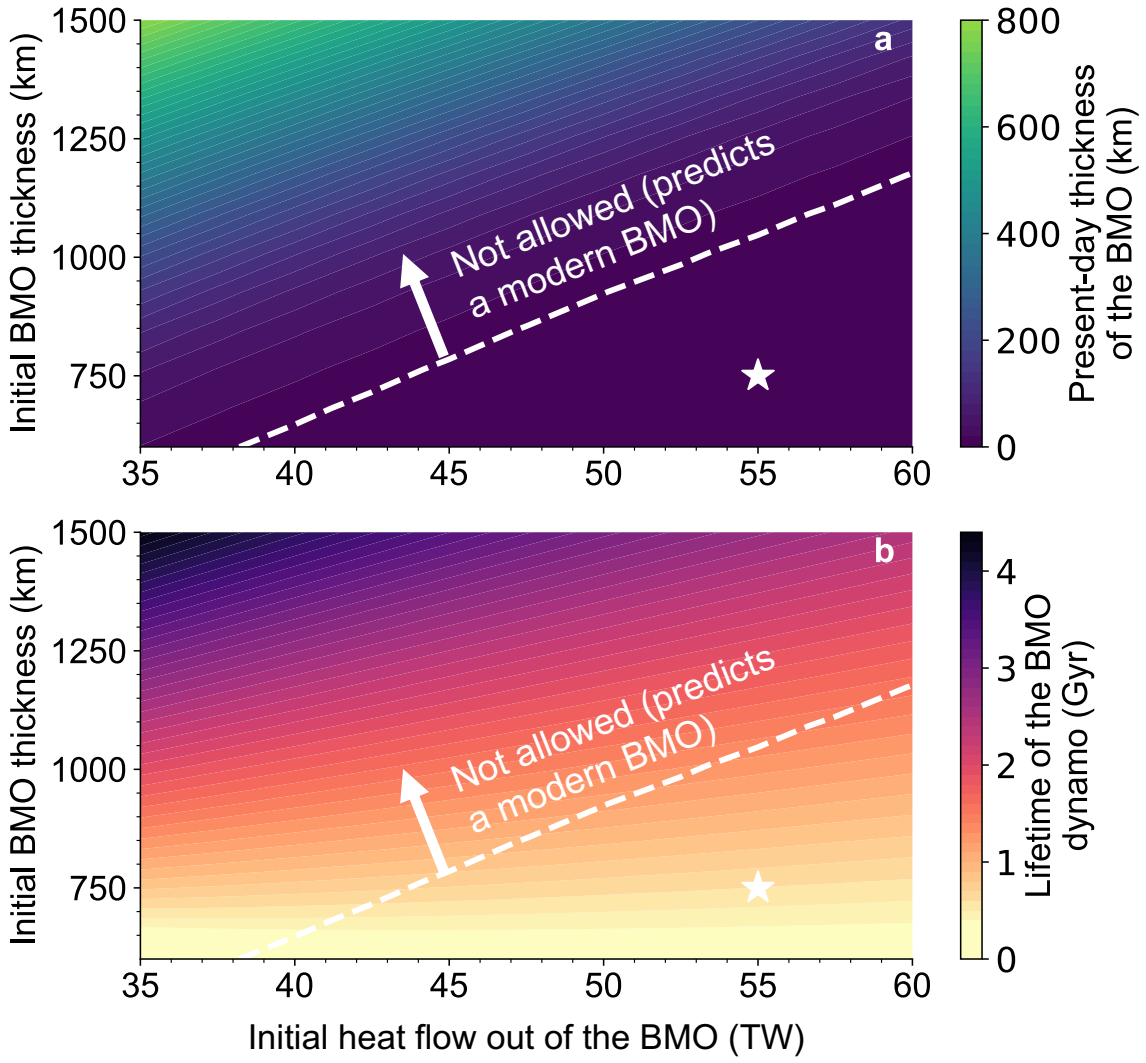

Figure S2. Sensitivity analysis for Earth discussed in Section 3.1 of the main text. The initial thickness of the basal magma ocean could have been ~1000 km or larger. Models with a thicker basal magma ocean conflict with seismic evidence against a global melt layer in the basal mantle. Arrows point towards invalid initial conditions on one side of the dashed white lines. (a) Present-day thickness of the basal magma ocean. (b) Lifetime of the dynamo in the basal magma ocean according to the Coriolis-Inertial-Archimedean scaling for flow velocity.

196

Variable	Value	Unit	Description
Basal magma ocean			
C_M	1000	J/K/kg	Specific heat of the basal magma ocean
ΔS_M	652	J/K/kg	Entropy of melting for the basal magma ocean
$\Delta\phi$	0.088		Change in mass fraction of Fe-rich component upon freezing
T_A	5500	K	Melting temperature of the Fe-rich component
T_B	3500	K	Melting temperature of the Mg-rich component
α_M	1.25×10^{-5}	1/K	Coefficient of thermal expansion in the basal magma ocean
σ_M	2×10^{4}	S/M	Electrical conductivity of the basal magma ocean
ε	0.63		Prefactor in the scaling law for a dynamo in the basal magma ocean
f_{ohm}	0.9		Fraction of available power that is converted into a dynamo
λ_M	1.38×10^{-17}	1/s	Average decay constant for radiogenic heating in the basal magma ocean
Core			
C_C	750	J/K/kg	Specific heat of the core
ΔS_C	127	J/K/kg	Entropy of melting for the core
γ	1.5		Grüneisen parameter
α_I	0.83		Coefficient of compositional expansion (inner core)
α_P	0.80		Coefficient of compositional expansion (light elements)
c_0	0.056		Initial mass fraction of light elements in the core
dT_L/dc	-21×10^{-3}	K	Change in liquidus temperature with composition
dT_L/dP	9×10^{-9}	K/Pa	Change in liquidus temperature with pressure
λ_C	1.76×10^{-17}	1/s	Average decay constant for radiogenic heating
H_K	4.2×10^{-14}	W/kg/ppm	Initial amount of radiogenic heating per unit mass per ppm of potassium
P_C	5×10^{-6}	1/K	Precipitation rate of light elements such as MgO and/or SiO_2 from the core

197 **Table S1.** Parameters that are held constant for both Earth and Venus. Values are taken from
198 Labrosse et al. (2007) for the basal magma ocean and from O'Rourke et al. (2018) for the core
199 unless otherwise noted in Text S1 or the main text.

Variable	Earth	Venus	Unit	Description
Planet				
r_P	6371	6052	km	Radius of the planet
Ω	7.27×10^{-5}	2.99×10^{-7}	1/s	Planetary rotation rate
Basal Magma Ocean				
H_T	7504	8699	km	Thermal scale height of the basal magma ocean
ρ_M	5500	5500	kg/m^3	Density of the basal magma ocean
Core				
r_C	3480	3110	km	Radius of the core
g	10.7	9.2	m/s^2	Gravitational acceleration near the core/mantle boundary
M_C	1.94×10^{24}	1.33×10^{24}	kg	Mass of the core
ρ_0	12451	11776	kg/m^3	Central density in the core
K	1403	1172	GPa	Effective modulus
K'	3.567	3.567		Derivative of the effective modulus
L_p	8049	7778	km	Length scale in the density profile
A_p	0.4835	0.4835		Constant in the density profile
P_C	125	130	GPa	Pressure at the core/mantle boundary
P_0	426	341	GPa	Effective central pressure
$T_L(0)$	5806	5124	K	Liquidus temperature at the center

Table S2. Parameters that are adjusted for application to Earth versus Venus, primarily to reflect the slight differences in internal pressures. Unless otherwise noted in Text S1 or the main text, values are taken from Labrosse et al. (2007) for Earth and O'Rourke et al. (2018) for Venus.

Variable	Units	Description
Basal Magma Ocean		
r_B	km	Radius of the upper boundary of the basal magma ocean
h_M	km	Thickness of the basal magma ocean
M_M	kg	Mass of the basal magma ocean
Q_{BMO}	TW	Heat flow out of the basal magma ocean into the solid mantle
Q_{SM}	TW	Secular cooling of the basal magma ocean
Q_{LM}	TW	Latent heat of solidification in the basal magma ocean
Q_{RM}	TW	Radiogenic heat in the basal magma ocean
T_M	K	Temperature of the solid mantle above the thermal boundary layer
T_C	K	Temperature of the basal magma ocean and uppermost core
v_M	m/s	Convective velocity in the basal magma ocean
Core		
r_I	km	Radius of the inner core boundary
T_{DC}	K	Average temperature in the outer core
T_{SC}	K	Effective temperature for dissipation from secular cooling
$T_L(r_I)$	K	Liquidus temperature at the inner core boundary
$[K]_C$	ppm	Abundance of potassium in the core
E_K	W/K	Entropy sink associated with thermal conduction
Q_{CMB}	TW	Total heat flow across the core/mantle boundary
Q_{SC}	TW	Secular cooling of the core
Q_{RC}	TW	Radiogenic heat in the core
Q_{PC}	TW	Gravitational energy from precipitation of light elements
Q_{GC}	TW	Gravitational energy from exclusion of light elements from the inner core
Q_{LC}	TW	Latent heat from the inner core
Q_{IC}	TW	Conductive cooling of the inner core
TDM	A m^2	True dipole moment of the core-generated magnetic field

Table S3. Key parameters that are tracked for the evolution of the basal magma ocean and core, which are defined in Text S1 and/or the main text.